15th Triennial World Congress, Barcelona, Spain

CONVERGENCE OF A SWITCHED HAMILTONIAN OBSERVER APPLIED TO AN SLR CONVERTER

Hultgren A.* Lenells M.**

* University of Kalmar, Department of Technology, Kalmar, Sweden
** Växjö university, School of Mathematics and Systems Engineering, Växjö, Sweden

Abstract: A design method for switched observers is presented. Global convergence of the switched observer is addressed in the case of a persistently exciting control signal. Hamiltonian modelling is used in the observer design. The observer is applied to a Series Loaded Resonant converter. A global model of the converter is given. Simulation is performed for illustration of the convergence properties.

Keywords: Convergence of observer, Switched systems, Lyaponov methods, Nonlinear analysis, Converter, Modelling.

1. INTRODUCTION

A design method for non-linear observers is presented. Global convergence of a switched observer is discussed in the case of a persistently exciting control signal. Some steps, what is believed, toward a convergence proof are presented. Hamiltonian modelling is used in the observer design. The observer is applied to a Series Loaded Resonant, SLR, converter. The SLR converter, see Fig. 2, is described in section two by a Hamiltonian state space description

$$\dot{x}(t) = [J(x) - R]\,\frac{\partial H}{\partial x}(x) + B(x)u(t),$$
$$y(t) = B(x)^T \frac{\partial H}{\partial x}(x),$$

where $J(x)$ is a skew-symmetric structure matrix, R is a positive semi-definite symmetric matrix possibly dependent on x, and $H(x)$ is the Hamiltonian function. Hamiltonian modelling of switched electric circuits of different topologies has been introduced by Escobar et al (1999) and Ortega et al (1998).

The switched nature of the converter and the observer depends on the division of the state space X in three subspaces Ω_i, $i \in \{-1, 0, 1\}$, see Fig. 1 and sec.2.1.1. In each of these subspaces the function

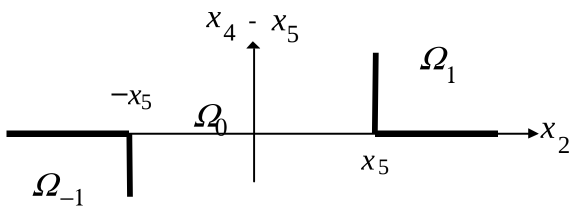

Fig. 1. Division of the state space X in three subspaces Ω_i, $i \in \{-1, 0, 1\}$

$J(x)$ is a constant matrix. Choosing $u(t)$ to be the applied voltage across the resonant circuit, $V_{AB}(t)$, implies that the function $B(x)$ is constant. Following a trajectory, $x(t)$, the description will switch between the three linear models each time the trajectory passes from one area Ω_i to another area Ω_j, $i \neq j$. Such a system is said to be a switched system.

The analysed SLR converter is shown in Fig. 2. Basic analysis of resonant converters can be found in Erickson and Maksimovi´c (1995) and Oruganti and Lee (1984). The SLR converter has many advantages over the conventional converters controlled with pulse width modulation, such as low switching losses at higher switching frequencies (zero-current switching, ZCS, or zero-voltage switching, ZVS), easier electromagnetic interference (EMI) filtering, and reduced switching stresses. The SLR converter is applied in a high voltage equipment with a capacitive load property. The transformer in the resonant circuit makes a significant contribution to the dynamics. The high number of windings on the secondary side of the transformer gives a high leakage capacitance, C_w. The capacitive load and the high transformer ratio, n, will give a comparatively large load capacitance, $C_L >> C_w$, $C_L >> C_r$, making the load voltage, V_0, only slowly varying. The converter is controlled by four IGBT transistors Z1-Z4 determining the voltage across the resonant circuit, V_{AB}, between junctions A and B.

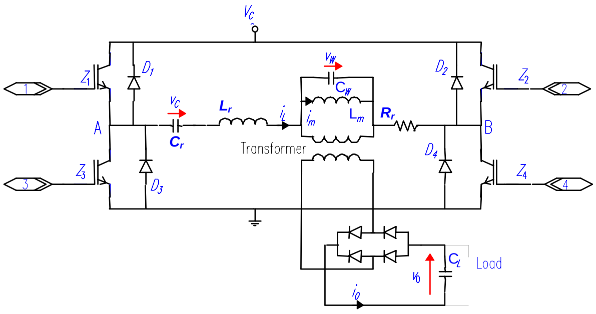

Fig. 2. The Series Loaded Resonant Converter

The presented result is part of a larger work of developing a controller for the SLR converter. The controller will be based on the states of the system due to demands of high bandwidth both in the servo function and in the regulator function. To allow control by state feedback, different observers have been developed. A switched Kalman filter experiment is reported in Hultgren et. al. (1999). In this report Kalman filter design is used for each linear subsystem. The filter performed well in simulations as well in practical experiments. However, it is hard to analyse global stability. The large changings of the system matrix and the noisy environment makes that it is believed that the approach of high gain observer is not applicable.

In the following section, the SLR converter is modelled by port controlled generalised Hamiltonian modelling. In section 3 the design of the proposed switched Hamiltonian observer is presented together with a discussion of observer stability. The issue of global convergence of the estimates is treated in more details in Hultgren and Lenells (submitted 2001). In the 4th section some simulation showing the observer convergence are presented. The conclusions are presented in the last section.

2. HAMILTONIAN MODELLING

To be able to use Hamiltonian modelling for global characterization of the complete SLR converter we have to use generalised Hamiltonian modelling. Consider the Hamiltonian formulation without energy dissipation

$$\begin{pmatrix} \dot{q}(t) \\ \dot{p}(t) \end{pmatrix} = J \begin{pmatrix} \dfrac{\partial}{\partial q} H(q,p) \\ \dfrac{\partial}{\partial p} H(q,p) \end{pmatrix} + \begin{pmatrix} 0 \\ G(q) \end{pmatrix} u(t),$$

where $J = \begin{pmatrix} 0 & I \\ -I & 0 \end{pmatrix}$ and $G(q)u(t) = \tau(t)$ is the generalised force acting on the system. Add the equation

$y(t) = G^T(q)\frac{\partial}{\partial p}H(q,p) = G^T(q)\dot{q}(t).$

Then the power fed to the system is

$u(t)^T y(t) = \tau^T(t)(G^T(q))^{-1}G^T(q)\dot{q}(t) = \tau^T(t)\dot{q}(t),$

and the power balance of the system is

$$\frac{dH}{dt} = \begin{pmatrix} \dfrac{\partial}{\partial q}H^T & \dfrac{\partial}{\partial p}H^T \end{pmatrix} \begin{pmatrix} \dot{q} \\ \dot{p} \end{pmatrix} = y(t)^T u(t).$$

The class of Hamiltonian systems can be generalised to systems described in local coordinates as

$\dot{x}(t) = J(x)\frac{\partial H}{\partial x}(x) + B(x)u(t),$

$y(t) = B^T(x)\frac{\partial H}{\partial x}(x),$

where $J(x)$ is the skew-symmetric structure matrix.

In this generalised case the number of capacitors and inductors in a circuit can be different giving an odd number of states in the generalised Hamiltonian model.

Energy dissipation can be included in the port-controlled Hamiltonian systems by terminating some of the ports using resistive elements giving the model structure of a **port-controlled Hamiltonian system with dissipation**

$\dot{x}(t) = [J(x) - R(x)]\frac{\partial H}{\partial x}(x) + B(x)u(t),$

$y(t) = B^T(x)\frac{\partial H}{\partial x}(x),$

where $R(x)$ is the positive semi-definite symmetric dissipation matrix.

The power balance is given by

$\frac{dH}{dt}(x(t)) = y(t)^T u(t) - \frac{\partial H}{\partial x}^T(x(t))R(x(t))\frac{\partial H}{\partial x}(x(t)).$

2.1 Modelling the converter

The Hamiltonian modelling starts with the storage function, $H(x)$, giving the energy of the system as a function of the states. In electric circuits a natural choice of state variables are the charges on the capacitors, q_i, and the magnetic flows in the inductors, φ_i. The gradient vector, $\partial H/\partial x$, and the circuit topology give information to parametrize the skew-symmetric structure matrix, $J(x)$, the energy dissipation matrix, R, and the control matrix, B.

2.1.1. Hamiltonian states

It is possible to find a global Hamiltonian model for the SLR converter, covering all the subspaces. The energy storing components in the circuit are the capacitances C_r, C_w, and C_L and the inductances L_r and L_m. The total storage function is given by:

$$H(q_r, q_w, q_L, \varphi_r, \varphi_m) =$$
$$\frac{1}{2}(\frac{q_r^2}{C_r} + \frac{q_w^2}{C_w} + \frac{q_L^2}{C_L} + \frac{\varphi_r^2}{L_r} + \frac{\varphi_m^2}{L_m}) = \frac{1}{2}x^T(t)Dx(t),$$

where $x^T = \begin{pmatrix} q_r & q_w & q_L & \varphi_r & \varphi_m \end{pmatrix}$ and $D^{-1} = diag(C_r, C_w, C_L, L_r, L_m)$.

The physical interpretation of the gradient vector, $\partial H/\partial x$, of the storage function is

$$\frac{\partial H}{\partial x} = \begin{pmatrix} \frac{\partial H}{\partial q_r}^T & \frac{\partial H}{\partial q_w}^T & \frac{\partial H}{\partial q_L}^T & \frac{\partial H}{\partial \varphi_r}^T & \frac{\partial H}{\partial \varphi_m}^T \end{pmatrix}^T$$

$$= Dx = \begin{pmatrix} \text{voltage across } C_r \\ \text{voltage across } C_w \\ \text{voltage across } C_L \\ \text{current through } L_r \\ \text{current through } L_m \end{pmatrix}.$$

The derivative of the state variables according to the Hamiltonian modelling is

$$\dot{x}(t) = \begin{pmatrix} \dot{q}_r \\ \dot{q}_w \\ \dot{q}_L \\ \dot{\varphi}_r \\ \dot{\varphi}_m \end{pmatrix} = \begin{pmatrix} \text{current through } C_r \\ \text{current through } C_w \\ \text{current through } C_L \\ \text{voltage across } L_r \\ \text{voltage across } L_m \end{pmatrix}.$$

2.1.2. State subspaces

The circuit operates in three different modes. Each mode corresponds to a conducting state of the rectifier. The rectifier has three possible conducting states; not conducting, conducting in positive direction and conducting in negative direction. Each of the conducting states corresponds to one of three different subspaces, Ω_s, where $s \in \{-1, 0, 1\}$ of the state space system:

Ω_1, pos. cond.: $\frac{\partial H}{\partial q_L} \leq \frac{\partial H}{\partial q_w} \wedge \frac{\partial H}{\partial \varphi_r} > \frac{\partial H}{\partial \varphi_m}$,

Ω_0, not cond.: $-\frac{\partial H}{\partial q_L} < \frac{\partial H}{\partial q_w} < \frac{\partial H}{\partial q_L}$,

Ω_{-1}, neg. cond.: $\frac{\partial H}{\partial q_w} \leq -\frac{\partial H}{\partial q_L} \wedge \frac{\partial H}{\partial \varphi_r} < \frac{\partial H}{\partial \varphi_m}$.

As has been written above, $J(x)$ is constant in each of the subspaces, this motivates the notation $J(s)$, $s \in \{-1, 0, 1\}$, where $s = -1$ when $x \in \Omega_{-1}$ etc..

2.1.3. Modelling

The modelling is straight forward in the subspace Ω_0. In the subspaces Ω_1, and Ω_{-1} the modelling is more delicate. Here we describe the modelling in Ω_1 in more detail.

In Ω_1 the load is connected via the rectifier in parallel with the winding capacitance, C_w, and the magnetising inductance L_m. Kirchhoffs laws give the following two equations, the first for the node connecting the resonant inductor and the transformer and the second for the parallel connection of C_w and C_L: $\dot{q}_w + \dot{q}_L = \frac{\varphi_r}{L_r} - \frac{\varphi_m}{L_m}$, $\frac{q_w}{C_w} = \frac{q_L}{C_L}$ and $\frac{\dot{q}_w}{C_w} = \frac{\dot{q}_L}{C_L}$. These equations imply: $\dot{q}_w = \frac{C_w}{C_w + C_L}\left(\frac{\varphi_r}{L_r} - \frac{\varphi_m}{L_m}\right)$, which is the second equation in the state model below. In a similar way the third row is derived. The circuit topology gives some freedom, $0 \leq \alpha \leq 1$, for the $\dot{\varphi}_r$ equation:

$$\dot{\varphi}_r = \frac{q_r}{C_r} - (1-\alpha)\frac{q_w}{C_w} - \alpha\frac{q_L}{C_L} - R_r\varphi_r + V_{AB}.$$

There is a similar freedom for the $\dot{\varphi}_m$ equation. By choosing $\alpha = I = \frac{C_L}{C_w + C_L}$ this freedom is used to shape a skew-symmetric matrix

$$J(1) = \begin{pmatrix} 0 & 0 & 0 & 1 & 0 \\ 0 & 0 & 0 & 1-I & -(1-I) \\ 0 & 0 & 0 & I & -I \\ -1 & -(1-I) & -I & 0 & 0 \\ 0 & 1-I & I & 0 & 0 \end{pmatrix}.$$

The modelling in Ω_{-1} is made under similar considerations. It is possible to formulate a global model, as shown in the next subsection

2.1.4. Global model

A global model is:

$$\dot{x}(t) = (J(s) - R)\,Dx(t) + BV_{AB}(t),$$

where $s \in \{-1, 0, 1\}$, and s is defined in 2.1.2 and

$$J(s) =$$
$$\begin{pmatrix} 0 & 0 & 0 & 1 & 0 \\ 0 & 0 & 0 & 1-s^2I & -\left(1-s^2I\right) \\ 0 & 0 & 0 & sI & -sI \\ -1 & -\left(1-s^2I\right) & -sI & 0 & 0 \\ 0 & 1-s^2I & sI & 0 & 0 \end{pmatrix},$$

$$R = \begin{pmatrix} 0&0&0&0&0 \\ 0&0&0&0&0 \\ 0&0&0&0&0 \\ 0&0&0&R_r&0 \\ 0&0&0&0&0 \end{pmatrix}, \text{ and } B = \begin{pmatrix} 0 \\ 0 \\ 0 \\ 1 \\ 0 \end{pmatrix}.$$

2.1.5. Controllability, observability and minimal realisations of the system

There is a need for five states in Ω_0. However, in Ω_{-1} and Ω_1 it is sufficient with four states. It is strongly believed that the use of five states in all subspaces makes the modelling more clear. However it can be seen that with the control signal matrix $B = \begin{pmatrix} 0 & 0 & 0 & 1 & 0 \end{pmatrix}^T$ the system is not controllable in any subspace. In Ω_0 the load is physically disconnected from the control signal. In the subspaces Ω_1 and Ω_{-1} the states of the capacitances C_w and C_L are dependent due to that the capacitors are parallel connected. It can also be seen that with a suggested measurement signal matrix $C = \begin{pmatrix} 0 & 0 & 0 & cL_r & 0 \end{pmatrix}$ the system is not observable in Ω_0 because the load is physically disconnected from the measurement of the system. In Ω_1 and Ω_{-1} the system can be described by a fourth order system and will then be observable.

The chosen realisation is a minimal one in the sense that the model should be able to track all the states in the switched system. In fact the use of five states in the model has been a crucial step taken in order to make a global model.

3. SWITCHED HAMILTONIAN OBSERVER

The states are estimated with a switched Hamiltonian observer. The measurement signal, $y(t)$, is the resonant current which is proportional to the magnetic flow in the resonant inductance, $y(t) = c\varphi_r(t)$. The process is given by

$\frac{dx(t)}{dt} = (J(s) - R)\, Dx(t) + Bu_{AB}(t),\ s \in \{-1, 0, 1\}$,

$y(t) = Cx(t)$, where $C = \begin{pmatrix} 0 & 0 & 0 & c & 0 \end{pmatrix}$.

The observer is given by

$\frac{d\hat{x}(t)}{dt} = (J(\sigma) - R)\, D\hat{x}(t) + K(\sigma)C\,(x(t) - \hat{x}(t)) + Bu_{AB}(t),\ \sigma \in \{-1, 0, 1\}$,

where $K^T(\sigma) = \begin{pmatrix} k_1(\sigma) & k_2(\sigma) & k_3(\sigma) & k_4(\sigma) & k_5(\sigma) \end{pmatrix}$ is the gain of the observer.

3.1 Convergence of the observer estimates

The convergence discussion of the observer is presented in two parts. The first part is under the condition that the switching is synchronous in the observer and in the process and the second part is when also asynchronous switching may occur. The convergence discussion is not complete, some mathematical subtilities will be adressed in Hultgren and Lenells (submitted 2001), for instance the existens of solutions.

3.1.1. Synchronous switching

Under the condition that the switching in the observer is synchronous with the switching in the process, $\sigma = s$, the derivative of the estimation error, $e(t) = x(t) - \hat{x}(t)$, is given by

$\frac{de(t)}{dt} = ((J(s) - R)\, D - K(s)C)\, e(t) =$

$((J(s) - R) - K(s)C_D)\, De(t)$,

where $C_D = \begin{pmatrix} 0 & 0 & 0 & cL_r & 0 \end{pmatrix}$.

A natural choice of a Lyapunov function is the energy-like function, compare the definition of H in section 2.1.1 above,

$V(e(t)) = \frac{1}{2}e(t)^T De(t)$.

$V : R^5 \to R$, $V(0) = 0$, and $V(e) > 0$ when $e \neq 0$. Assume V is regular enough. If $e = 0$ is an equilibrium point, Lyaponov stability theorem tells that a sufficient condition for stability of $e(t)$ is that $\frac{dV(e(t))}{dt} \leq 0$ (Khalil 1996).

The derivative of the Lyapunov function is

$\frac{dV(e(t))}{dt} =$

$-\frac{1}{2}e(t)^T D\left[2R + C_D^T K^T(s) + K(s)C_D\right] De(t)$.

A sufficient condition for stability of $e(t)$ is

$\left(2R + C_D^T K^T(s) + K(s)C_D\right) \geq 0$.

This expression can be used to design the observer.

Apparently $R \geq 0$. If $k_4(s)cL_r > -R_r$ and $k_1(s) = k_2(s) = k_3(s) = k_5(s) = 0$ then $\frac{dV(e(t))}{dt} = -\frac{1}{2}\left(2k_4(s)cL_r + 2R_r\right)\left(\frac{e_4}{L_r}\right)^2 \leq 0$.

We believe, see Hultgren and Lenells (submitted 2001), that the LaSalle's theorem (Khalil 1996) can be used in order to prove global convergence in the case the control works in normal mode. This means that the system runs in a cycle: $(\Omega_{-1}, \Omega_0, \Omega_1, \Omega_0, \Omega_{-1}, ...)$.

3.1.2. Asynchronous switching

When running the observer there will be estimation errors, hence there is mostly asynchronous switching.

The derivative of the Lyapunov function is in this case given by

$$\frac{dV(e(t))}{dt} = -\frac{1}{2}e(t)^T D[2R + C_D^T K^T(\sigma) + K(\sigma)C_D]De(t) + \Delta_{s,\sigma}.$$

The first term is the same as in the synchronous case. Below it is shown that the second term $\Delta_{s,\sigma}$ is negative definite and this will imply that the estimates will converge also in the case of asynchronous switching.

$\Delta_{s,\sigma} = e^T D\,[J(s) - J(\sigma)]\, D\hat{x}$ where

$s, \sigma \in \{-1, 0, 1\}$.

$\Delta_{s,\sigma} = I\left(s^2 - \sigma^2\right)[(e_4 - e_5)\,\hat{x}_2 + (\hat{x}_5 - \hat{x}_4)\, e_2]$

$+ (s - \sigma)\,[(e_5 - e_4)\,\hat{x}_3 + e_3\,(\hat{x}_4 - \hat{x}_5)]$.

Defining

$Dx^T = \begin{pmatrix} u_r & u_w & u_L & i_r & i_m \end{pmatrix}$, and

$D\hat{x}^T = \begin{pmatrix} v_r & v_w & v_L & j_r & j_m \end{pmatrix}$,

it follows that

$\frac{\Delta_{s,\sigma}}{I} = (s - \sigma)\,[(i_r - i_m)\,((s + \sigma)\, v_w - v_L) -$

$(j_r - j_m)\,((s + \sigma)\, u_w - u_L)]$.

When calculating the value of $\Delta_{s,\sigma}$ the following equations are needed:

for $s = 0$, not conducting mode, $\dot{q}_L = 0$, $u_L > 0$ and $-u_L < u_w < u_L$,

for $s = 1$, positive conducting mode, $\dot{q}_L > 0$, $\dot{q}_L = I(i_r - i_m)$ and $u_L = u_w \geq 0$,

for $s = -1$, negative conducting mode, $\dot{q}_L > 0$, $\dot{q}_L = -I(i_r - i_m)$ and $u_L = -u_w \geq 0$.

There are corresponding relations for the observer, $\sigma \in \{1, 0, -1\}$.

3.1.3. Study of $\Delta_{s,\sigma}$ It can be shown that the disturbance term $\Delta_{s,\sigma} < 0$ for all $s, \sigma \in \{-1, 0, 1\}, s \neq \sigma$. Here we only present the case when $s = 1$ and $\sigma = 0$,

$$\Delta_{1,0} = (i_r - i_m)(v_w - v_L) + (j_r - j_m)(u_L - u_w) < 0.$$

This holds because $s = 1$ implies $u_L = u_w$, and $i_r - i_m > 0$, and $\sigma = 0$ implies $v_w < v_L$. The negative definiteness of the other five cases can be shown in a similar way.

The negative definiteness of dV/dt at asynchronous switching means that there are no invariant solutions in the case of asynchronous switching, implying that the invariant solutions have to be found in the synchronous switching case. This indicates that if the observer converge in the synchronous case it will also converge in the asynchronous case.

Observe that the estimates converge also in the case when $R = 0$ and $K = 0$.

4. SIMULATIONS

Some simulations are shown for illustration of the convergence result. First some simulations are shown with initial errors in e_1, e_2, e_4, and e_5, Fig. 3 - Fig. 8. At last one simulation is shown with an initial error also in e_3, Fig. 9. In that case the convergence is much slower due to the very large capacitance in the load, it is about 500 times larger than the resonance capacitance. The simulation parameters are, see Fig. 2, $V_C = 500$, $C_r = 2\mu F$, $R = 0$, $L_r = 32\mu H$, $L_m = 300\mu H$, $C_w = 200nF$, and $C_L = 1mF$.

In Fig. 3 and Fig. 4 the Lyaponov function and the estimation errors are presented in the case of zero Hamiltonian observer gain, $K = 0$. The convergence here only depends on the $\Delta_{s,\sigma}$-term. In Fig. 5 the process values in this simulation can be seen. The design $k_4(s)cL_r > -R_r$ and $k_1(s) = k_2(s) = k_3(s) = k_5(s) = 0$ is presented in Fig. 6 and Fig. 7. The convergence of the observer in the case when the rectifier is conducting and the observer model of the rectifier is conducting in the opposite direction is shown in Fig. 8.

In Fig. 3, 6, 8, and 9 is $s - \sigma$ plotted, hence it is possible to see when the estimator and the process are described by the same model or by different models.

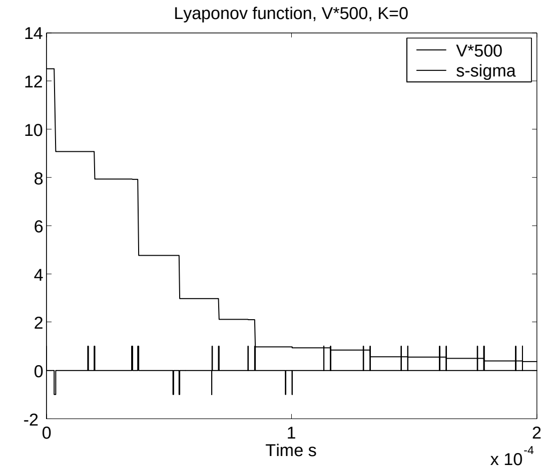

Fig. 3. The Lyapunov function, V·500.

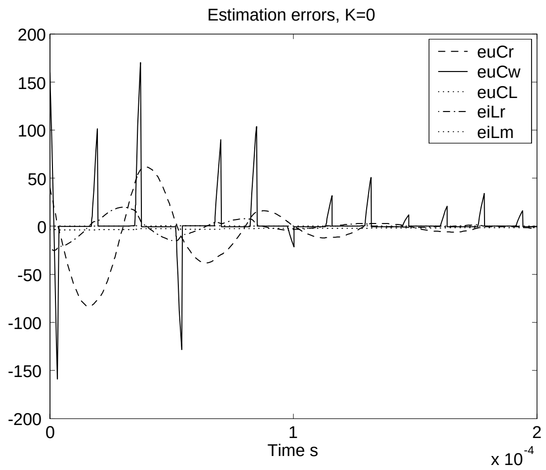

Fig. 4. The estimation errors, K=0.

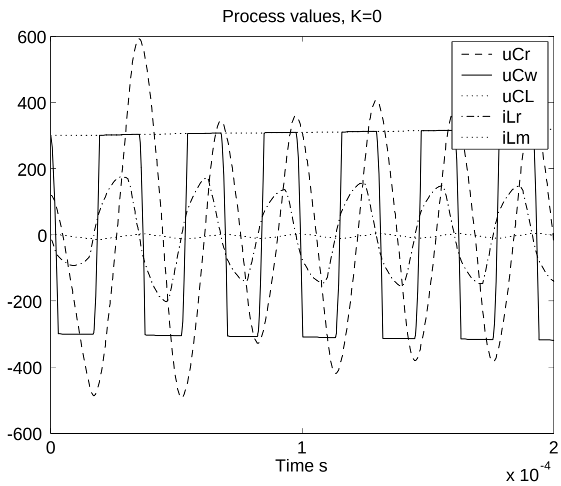

Fig. 5. Process values in the simulation.

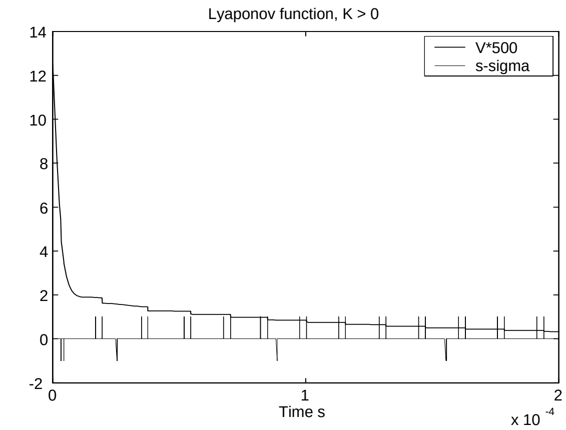

Fig. 6. The Lyaponov function, $V \cdot 500$. $K > 0$.

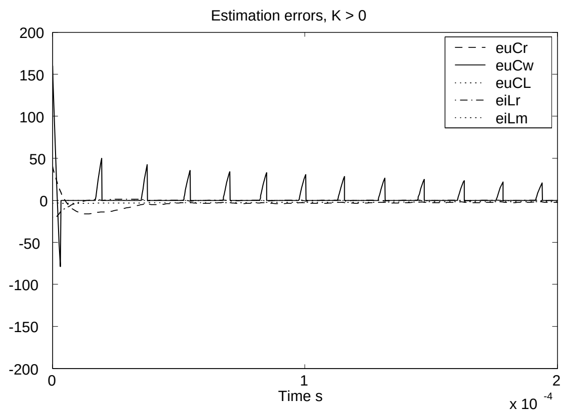

Fig. 7. The estimation errors, $K > 0$.

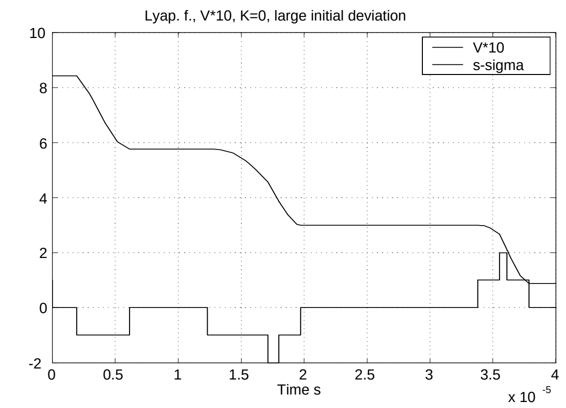

Fig. 8. The Lyaponov function, $V \cdot 10$. $K = 0$.

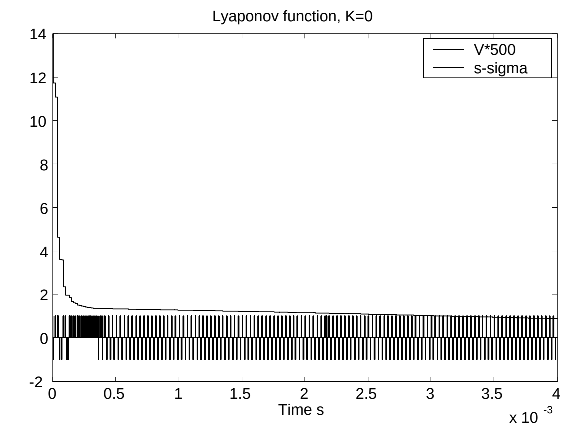

Fig. 9. Lyaponov function, $V \cdot 500$.

5. CONCLUSION AND FUTURE WORK

Hamiltonian modelling combined with Lyaponov theory can be used for convergence analysis and observer design for the switched series loaded resonant converter. Hamiltonian modelling gives natural candidates for Lyaponov functions.

It is possible to give a global model of the SLR converter by use of the Hamiltonian method.

The treated nonlinear observer converge also in the case when $R = 0$ and $K = 0$. This is not true in the linear case, $s = \sigma$. This can be seen for instance in Fig. 8, There V is constant when $s = \sigma$, which means that the process and the observer are described by the same linear model.

Future work will be devoted to generalise the result of this report and give it as a mathematical theorem. We will also try to design a controller for the resonant converter by use of the method of this report.

6. REFERENCES

Erickson, R. W., Maksimović, D. Fundamentals of power electronics, second edition, Kluwer Academic Publishers, 1999.

Escobar, G., Van der Schaft, A. J., Ortega, R., A Hamiltonian viewpoint in the modeling of switching power converters, Automatica 35 (1999), 445-452

Hultgren, A., Kulesza, W., Lenells, M., Switched Kalman filter in a high frequency series loaded resonant converter, Proceeding of IEEE CCA conference 1999. Anchorage September 1999.

Hultgren, A. and Lenells M., Convergence of a switched Hamiltonian Observer Applied to an SLR converter. Submitted to Automatica,22 Sept 2001, as an augmented version of this article.

Khalil H. K., Nonlinear systems, Prentice-Hall, second edition, 1996.

Ortega R., Loria, A.,Nicklasson, P. J., and Hebertt, S. R., Passivity-based Control of Euler-Lagrange Systems, Springer, 1998.

Oruganti, R., Lee, F. C., Resonant Power Processors Part 1 - State Plane Analysis, Part II - Methods of Control, IEEE-IAS, annual meeting 1984.

van der Schaft, A., L_2-Gain and Passivity Techniques in Nonlinear Control, Springer, 2000.